Nuclear Engineering and Technology 58 (2026) 104296

Contents lists available at ScienceDirect

Nuclear Engineering and Technology

journal homepage: www.elsevier.com/locate/net

Original Article

Evaluation of long-term thermal durability of neutron-shielding resin in dry storage casks

Sia Hwang [a], Tae Uk Kang [b], Min Ji Kim [c], Woo Jun Kang [d], Hee Reyoung Kim [a,*]

[a] Department of Nuclear Engineering, Ulsan National Institute of Science and Technology (UNIST), Ulsan, 44919, Republic of Korea
[b] Agency for Defense Development, Daejeon, 34186, Republic of Korea
[c] Institute for Rare Isotope Science (IRIS), Institute for Basic Science (IBS), Daejeon 34000, Republic of Korea
[d] Dongwon EN-Tec Co., Ltd., Ulsan, 44992, Republic of Korea

ARTICLE INFO

Keywords:
Neutron shielding resin
Thermal durability
Dry storage cask
Long-term thermal test
Spent nuclear fuel

ABSTRACT

This study evaluated the long-term thermal durability of the neutron-shielding resin RNS-NR under long-term thermal exposure. RNS-NR was exposed to 170 °C in open-type and closed-type chambers, with weight loss monitored for 1500 h and material characterization conducted after 2000 h. TGA, XRD, and ICP-OES were used to evaluate thermal, structural, and compositional stability. After 1500 h, the weight-loss rate was 0.447 wt% in the closed-type chamber and 1.380 wt% in the open-type chamber, indicating greater volatile removal in the open configuration. TGA showed major decomposition at 262.54 °C, suggesting that the mass loss at 170 °C was dominated by moisture release rather than polymer degradation. XRD confirmed no detectable phase change of aluminum hydroxide after thermal exposure. ICP-OES analysis of the water-rich condensate collected from the closed-type chamber detected boron at 17.6 ppm and zinc at 188 ppm, while aluminum was not detected. These results indicated minor transfer of B and Zn into the condensate. Based on this observation, ICP-OES analysis of solid samples showed that the boron content decreased from 1.37 wt% to 0.60–0.30 wt% in the open-type chamber and to 0.48–0.31 wt% in the closed-type chamber, with retention dependent on sampling location.

1. Introduction

Spent nuclear fuel, generated during the operation of nuclear power plants (NPPs), exhibits high levels of radioactivity and heat generation, which require stringent safety management and long-term storage strategies. In Korea, spent nuclear fuel is temporarily stored at each NPP site using wet storage (pool-type storage facilities) and dry storage (dry cask storage systems). As of 2025, the cumulative inventory of spent nuclear fuel in Korea amounts to approximately 506,493 fuel assemblies, including about 23,721 assemblies from pressurized water reactors (PWRs) and 482,772 assemblies from heavy-water reactors (PHWRs). Among the PHWR assemblies, 81,012 are stored in wet storage and 401,760 are stored in dry storage facilities [1]. Currently, spent nuclear fuel from all PWRs in Korea is exclusively stored in wet storage. However, at the Wolsong site, temporary dry storage facilities were introduced at an early stage due to the rapid saturation of pool storage capacities. The introduction of dry storage at Wolsong was a strategic measure to address the storage challenges arising from PHWRs, which generate approximately four to five times more spent fuel per reactor compared to typical PWRs [1]. In Korea, approximately 400 tons of spent nuclear fuel are generated annually from 20 PWRs, which corresponds to about 20 tons per reactor. Additionally, around 350 tons are produced from four PHWRs, averaging approximately 90 tons per reactor per year [2]. At present, Wolsong remains the only site in Korea operating active dry storage facilities. Other PWR sites, such as Kori, Hanbit, Hanul, and Saeul, currently use wet storage exclusively; however, dry storage solutions are actively being pursued due to anticipated shortages of pool storage capacities. In addition to capacity limitations, wet storage systems require continuous operation of cooling, purification, and sampling systems, resulting in relatively high maintenance complexity and operational burdens.

In contrast, dry storage systems offer significant advantages in safety and operational simplicity, employing passive cooling mechanisms through natural convection. Typically, dry storage casks are constructed with outer shielding materials such as reinforced concrete or metallic shells and are internally filled with neutron-shielding materials. Commonly used neutron-shielding materials in commercial dry storage casks include borated polyethylene resin, solid borated polyester resin,

* Corresponding author.
E-mail address: kimhr@unist.ac.kr (H.R. Kim).

https://doi.org/10.1016/j.net.2026.104296
Received 22 October 2025; Received in revised form 17 March 2026; Accepted 23 March 2026
Available online 24 March 2026

and epoxy-based resins such as TN-9 and NS-4-FR [3,4]. Currently, dry cask storage technologies utilized or under consideration in Korea primarily depend on foreign technologies and suppliers. Major international vendors of neutron-shielding material include NAC International (NS-4-FR resin), TransNuclear (borated polystyrene resin), and HOLTEC International (borated polymer resin) [5]. These commercial neutron-shielding materials must comply with strict performance criteria defined by regulatory guidance documents such as the U.S. Nuclear Regulatory Commission (NRC)'s Standard Review Plans, notably NUREG-2215, Standard Review Plan for Spent Fuel Dry Storage Systems and Facilities, and NUREG-2216, Standard Review Plan for Transportation Packages for Spent Fuel and Radioactive Material [6,7]. According to these regulatory documents, safety analysis reports must detail how neutron-shielding performance might be affected under varying environmental conditions, such as elevated temperatures.

Elevated temperatures may reduce hydrogen content in shielding materials through the loss of bound or water-rich condensate, or polymer decomposition, which decreases material integrity [8]. Since spent nuclear fuel storage and transportation systems operate under prolonged elevated-temperature conditions, ensuring the long-term thermal stability and durability of neutron-shielding materials is critical. Thermal degradation or instability of these shielding materials can lead not only to reduced shielding efficiency but also to potential structural integrity issues within storage casks. Therefore, comprehensive and scientifically rigorous assessments of thermal stability and durability under long-term, high-temperature exposure conditions are required. In addition, in neutron-shielding resin composites, the spatial distribution of functional fillers is an important microstructural factor because well-dispersed shielding phases can increase the probability of radiation–material interactions and thereby influence shielding-related performance [9,10]. The recent studies emphasize that filler dispersion and agglomeration behavior should be examined together with thermal and mechanical stability because microstructural heterogeneity can affect composite durability under radiation protection conditions [11,12]. Based on these technical considerations, the present study aims to evaluate the thermal durability of neutron-shielding materials intended for long-term use in elevated-temperature environments. For this evaluation, RNS-NR, a representative neutron-shielding resin recently developed in Korea, was selected as the material for the case study. RNS-NR is the designation used by the manufacturer for this material and does not represent an abbreviation. The research specifically examines changes in weight, thermal degradation characteristics, and material property variations of RNS-NR under prolonged thermal exposure. Through this detailed analysis, the study provides fundamental scientific insights into the thermal stability and long-term performance reliability of neutron-shielding resins.

2. Materials and methods

2.1. Design of test cask for long-term thermal test

Dry storage casks for spent nuclear fuel use polymer-based neutron-shielding resins in their cask walls or overpacks to attenuate neutron radiation. These resins are designed to withstand the elevated temperatures caused by the decay heat of spent fuel, while remaining below their thermal degradation thresholds during normal operation. For example, Holtec's borated epoxy resin Holtite-A has a design temperature of about 300 °F (149 °C), and analyses must demonstrate that the resin's maximum normal operating temperature remains below this limit [13]. Commercial neutron-shielding materials currently in use have been evaluated for their long-term thermal durability under elevated temperature conditions ranging from 120 °C to 170 °C [14,15]. In this study, tests were conducted at the extreme temperature condition of 170 °C to accelerate the aging process and effectively assess the weight loss and degradation of RNS-NR under long-term thermal exposure.

The test duration of 1500 h was selected based on previous findings indicating a rapid weight change within the first 200 h and a relatively steady trend after 1000 h [15]. Therefore, this duration is sufficient to capture both the initial rapid degradation and the subsequent stable behavior of the material. By adopting the same time frame, a direct comparison of thermal degradation characteristics between RNS-NR and existing commercial materials can be achieved. The test cask for long-term thermal testing was designed to expose the neutron-shielding resin to a thermal environment of 170 °C for durations of 1500 h and 2000 h. At this temperature, two test setups were constructed: a closed-type chamber and an open-type chamber, as shown in Fig. 1. The exposure durations of 1500 h and 2000 h were selected to capture representative long-term weight loss behavior of the resin under these temperature conditions.

Fig. 2 shows the neutron-shielding resin filled into the test cask and illustrates the actual configuration and filling geometry used in the long-term thermal test. Under these conditions, the weight loss of the resin and the changes in material properties before and after thermal exposure were measured and analyzed to evaluate the long-term thermal stability of the neutron-shielding resin. The dry cask has an outer diameter of 2126 mm and an overall height of 5285 mm [16]. In the cross-sectional area available for the neutron-shielding resin, the thickness is approximately 100 mm, and the maximum thickness of the resin, free from interference by diagonal metal shells, is approximately 130 mm. Considering that the height of the neutron-shielding resin in the actual dry cask is 4644 mm, a scaled-down test setup was designed to accommodate a resin height of approximately 465 mm (1/10 scale), reflecting the heating direction and surrounding materials such as SUS304. Based on these requirements, a mold suitable for the specified resin dimensions and thermal conditions was designed and fabricated. For the test chambers, the closed-type chamber was specifically designed and manufactured to withstand internal pressure generated by water-rich condensate evaporating into steam during thermal testing. A pressure-resistance test confirms that the closed-type chamber could withstand an internal pressure of 1.50 MPa for 1 min. The inclusion of both open-type and closed-type chambers in this study aimed to evaluate the influence of water-rich condensate evaporation under different conditions. Specifically, the open-type setup allows direct contact with the ambient atmosphere, enabling continuous release of volatile components, whereas the closed-type configuration retains the evaporated water-rich condensate within the chamber. Accordingly, the chamber-wall thickness was set at 10 mm, and both closed-type and open-type neutron-shielding resin samples were fabricated with identical dimensions of 465 mm × 130 mm × 100 mm. Heater panels were mounted on one side of each chamber as flat plates to ensure even heat distribution across the entire surface area. These heater panels were capable of operating at temperatures up to 300 °C. Given the long-term operation period of 1500 h, temperature sensors were attached to each heater panel to continuously monitor and verify proper functioning. The temperature sensors were K-type thermocouples, selected for their

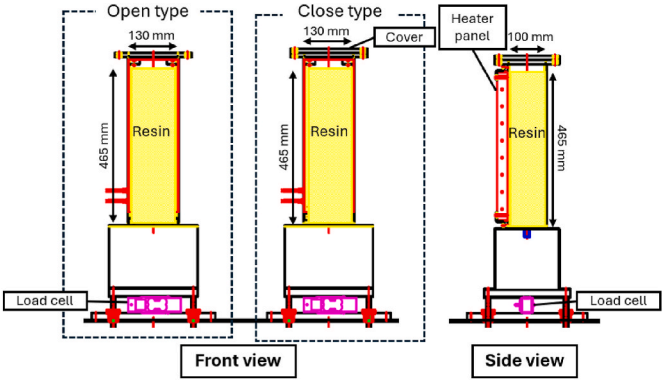

Fig. 1. Schematic diagrams of the test casks (open-type and closed-type).

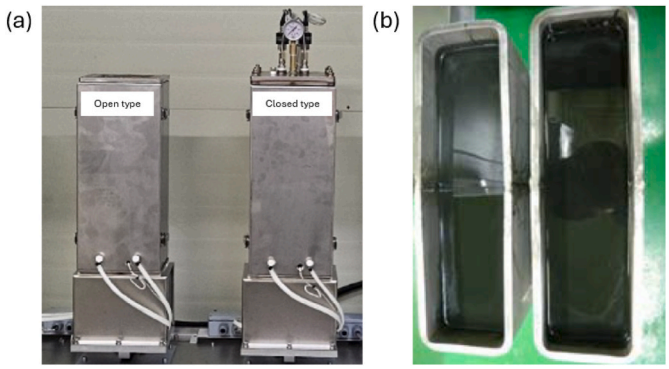

Fig. 2. Photographs of (a) the open-type and closed-type test casks and (b) the neutron-shielding resin filled into the casks.

stability over a wide temperature range and compliance with a Class 0.75 accuracy standard. For mass measurements, the chambers were designed to accommodate the maximum weight determined by the chamber structure and resin. The total expected mass, including the resin and auxiliary components, was approximately 40 kg. The load cell was rated for a maximum load of 60 kgf to adequately accommodate the anticipated maximum system mass. A load cell and an indicator with a resolution of 1 g were installed to detect mass variations, which were expected to remain within a 2% range during the long-term thermal durability test. Temperature and mass measurements were recorded at 1-h intervals throughout the test.

2.2. Neutron-shielding resin (RNS-NR)

RNS-NR consists of an epoxy resin and curing agent matrix, in which aluminum hydroxide, zinc borate, and boron carbide are incorporated as inorganic additives. The neutron-shielding resin RNS-NR was developed using a multi-material approach to achieve flame retardancy, thermal conductivity, and neutron attenuation. Aluminum hydroxide ($Al(OH)_3$, CAS No. 21645-51-2) served as the primary filler to provide base flame-retardant and heat-dissipation properties. Zinc borate ($ZnO{\cdot}xB_2O_3{\cdot}yH_2O$, $x > 0$ and $y > 0$, CAS No. 1332-07-6) acted as a secondary filler to enhance flame retardancy and contribute to neutron capture. Boron carbide (B_4C, CAS No. 12069-32-8) was added as an auxiliary filler to maximize neutron-shielding performance.

This combination of fillers was optimized for long-term thermal stability and effectiveness in dry-cask neutron shielding. RNS-NR also contains zinc borate and boron carbide to achieve neutron-shielding performance [17]. The primary component of the RNS-NR resin used in this study was aluminum hydroxide which served as the main filler. Aluminum hydroxide offers multiple benefits, particularly its flame-retardant functionality. During combustion, it releases water vapor, which dilutes oxygen concentration and suppresses flammable gases. It begins to thermally decompose at around 220 °C, absorbing heat and thereby lowering the surrounding temperature to inhibit flame propagation [18,19]. From an environmental standpoint, it is a halogen-free material that emits no toxic gases during combustion and demonstrates excellent dispersibility in a wide range of general polymers. In order to enhance flame-retardant and neutron-absorption performance, zinc borate was incorporated as a secondary filler. When used with aluminum hydroxide, zinc borate exhibits synergistic flame-retardant effects through a dehydration reaction [20]. It also functions as a smoke suppressant, improving visibility and safety during fire incidents. Its inclusion of boron oxide (B_2O_3) further enables thermal neutron capture, thereby improving the shielding effectiveness of the resin [21]. For additional neutron absorption and moderation capabilities, boron carbide was used. Boron carbide is a ceramic-based material with high boron content and is widely used in control rods of nuclear reactors because of its verified neutron-attenuation performance [22]. Through the optimal combination of these multifunctional fillers (aluminum hydroxide, zinc borate, and boron carbide), the RNS-NR resin was engineered to provide long-term thermal stability and enhanced neutron-shielding performance. This material was selected for experimental evaluation in the present study.

2.3. Analysis methods for resin

To evaluate the safety of the neutron-shielding resin, both physical and material property changes under elevated temperature conditions were examined. Thermogravimetric analysis (TGA) was performed to assess the thermal response of the resin using a Q500 instrument manufactured by TA Instruments. Based on prior studies, significant weight loss was expected to occur around 200 °C; therefore, the TGA test temperature range was set between 100 °C and 400 °C [14]. The sample was equilibrated at 100 °C and held isothermally for 1 min before heating. The temperature was increased from 100 °C to 400 °C at a ramp rate of 10 °C/min, followed by an isothermal hold of 1 min at 400 °C. To examine the microstructural distribution of inorganic fillers within the RNS-NR composite, scanning electron microscopy and energy-dispersive X-ray spectroscopy (SEM-EDS) were conducted on the cross section of the resin. The analysis qualitatively assessed the dispersion and spatial distribution of aluminum hydroxide, zinc borate, and boron carbide within the polymer matrix through elemental mapping of Al, O, Zn, and B. In particular, B was included in the EDS mapping because boron-bearing phases were responsible for neutron attenuation, and prior studies reported that improved dispersion of shielding fillers was an important microstructural indicator for interpreting shielding performance [9,10]. Cross-sectional specimens were mounted using a quick-set epoxy (powder:hardener = 2:1) and polished sequentially using SiC sandpapers (#320, #600, and #1200) followed by diamond suspensions (9 μm and 1 μm). Prior to SEM-EDS, the polished surfaces were Pt-coated (10 mA, 70 s). SEM-EDS analysis was performed using a Hitachi SU8600 instrument operated at an accelerating voltage of 15 kV with an Oxford EDS detector. To examine structural changes in the RNS-NR resin before and after long-term thermal exposure, X-ray diffraction (XRD) analysis was conducted. The samples were pulverized into powder form prior to analysis, which was performed using the EMPYREAN model diffractometer manufactured by Panalytical B.V. The scanning range, 2θ, was set from 10° to 80°. This test aimed to evaluate structural integrity at elevated temperatures by comparing diffraction patterns for any significant differences. The absence of notable changes between pre- and post-exposure patterns would indicate that the resin maintained structural stability even under prolonged high-temperature conditions. Phase identification of the resin samples was conducted by comparing the XRD patterns obtained with reference data from the PDF-4+ 2025 database [23]. Additionally, inductively coupled plasma optical emission spectrometry (ICP-OES) was conducted to quantify the boron (B) content in RNS-NR samples and water-rich condensate after thermal aging. For solid RNS-NR analysis, the resin was pulverized. The measurements were carried out using a 5100 ICP-OES instrument manufactured by Agilent Technologies. The 5 mL of nitric acid and 2 mL of hydrofluoric acid were added, and the mixture was digested using a microwave system (CEM Corporation, MARS 6) that ramped up to 170 °C and held for 20 min. After digestion, the solution was cooled down and used for ICP-OES analysis. Following thermal testing, a small amount of moisture condensed on the inner surface of the closed-type chamber, and a total of 3.67 g of water-rich condensate was collected. Because only a limited quantity of condensate was recovered, ICP-OES was selected because it enabled elemental analysis with small sample volumes. The collected water-rich condensate was analyzed by ICP-OES to identify inorganic species potentially released from the resin during heating. Al, B, and Zn were selected as target elements based on the primary and secondary filler constituents of RNS-NR. This analysis focused on determining whether long-term exposure to high temperatures resulted in any significant reduction in boron content (a key

element for neutron-shielding performance), thereby evaluating the chemical stability of the material. The XRD and ICP-OES analyses were performed using samples collected from three distinct positions within the test cask: the area closest to the heater panel, the center region, and the side section. This sampling approach was adopted to evaluate potential variations in material characteristics depending on proximity to the heat source. The weight-loss monitoring test was conducted for 1500 h. The 2000 h thermal exposure duration was selected to conservatively evaluate the cumulative effects of prolonged thermal aging on the structural integrity and chemical stability of the neutron-shielding resin. As shown in Fig. 3, sampling locations for XRD and ICP-OES analyses were defined in both the open-type and closed-type casks. Samples were collected from three representative positions: the region adjacent to the heater panel, the central region, and the side region. These sampling positions correspond to the central portion of the neutron-shielding resin, specifically a 105 mm section obtained by removing the upper and lower 180 mm regions from the total resin height of 465 mm. The extracted specimens were then sectioned at 5 mm intervals along the centerline to obtain representative samples for XRD and ICP-OES analyses. The two circular holes visible in Fig. 3 correspond to thermocouple insertion ports, which were used to place thermocouples at the mid-depth of the resin to verify stable heater operation during the 2000 h thermal exposure.

3. Results and discussion

3.1. Weight loss of neutron-shielding resin during the long-term thermal test

To evaluate the long-term thermal durability of the neutron-shielding resin, a thermal test system was designed to maintain a temperature of 170 °C for 1500 h, during which weight changes were continuously monitored to assess any potential effect on shielding effectiveness. As shown in Fig. 4 (a), the heater operated stably in both test chambers (open-type and closed-type), and the target temperature was consistently maintained throughout the test period. Fig. 4 (b) shows the weight variations for the open-type and closed-type chambers. No abrupt weight loss was observed under either condition. Over the 1500 h exposure at 170 °C, both samples exhibited a gradual and steady decrease in weight. In the closed-type chamber, the weight of the neutron-shielding resin decreased from 9627 g initially to 9584 g after 1500 h. In the open-type chamber, the weight declined from 9785 g to 9650 g. The greater weight loss in the open-type chamber is attributed to the continuous evaporation of water-rich condensate formed during heating, which escaped into the surrounding atmosphere. Minor fluctuations, including slight increases and decreases in measured weight, were observed during the test. However, the overall trend remained a gradual reduction. These fluctuations were not considered actual mass changes but were likely caused by air convection within the chamber, induced by the circulation system used for fire prevention.

The weight loss was determined by calculating the difference between the initial weight and the measured weight at each time point using equation (1). The weight-loss rate was calculated using equation (2), where W_t is the weight at a given time t, and W_0 is the initial weight. The initial weight was 9785 g for the open-type and 9627 g for the closed-type sample.

$$Weight\ loss = W_0 - W_t \tag{1}$$

$$Weight\ loss\ rate\ (wt\%) = \frac{W_0 - W_t}{W_0} \times 100 \tag{2}$$

Fig. 4 (c) and (d) show the weight loss and weight-loss rate as calculated using equations (1) and (2) for the open-type and closed-type chambers. The closed-type resin exhibited a total weight loss of 43 g (0.447 wt%) after 1500 h, whereas the open-type resin showed a loss of 135 g (1.380 wt%), representing approximately a threefold difference. Notably, the open-type sample displayed a weight loss rate more than twice that of the closed-type even in the early stages of testing, and the gap continued to widen over time. This trend can be attributed to the open structure allowing direct contact with ambient air, which

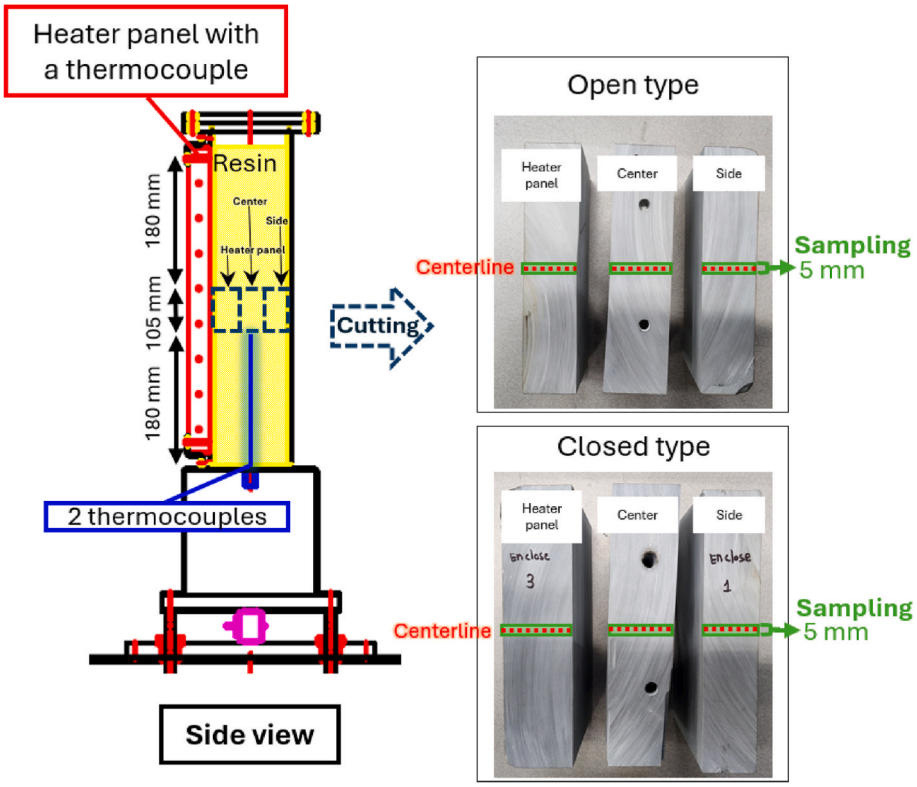

Fig. 3. Sampling locations for XRD and ICP-OES analysis in the neutron-shielding resin.

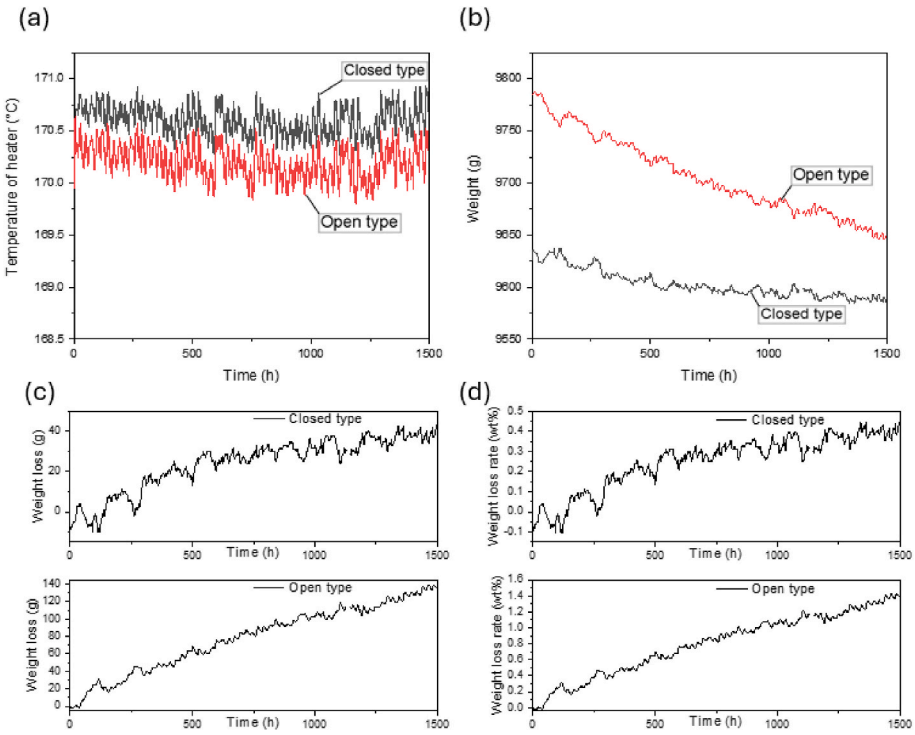

Fig. 4. (a) Heater temperatures in open-type and closed-type chambers; (b) Weight of neutron-shielding resin during 1500 h of thermal exposure at 170 °C; (c) Weight loss of the open and closed-type chambers; (d) Weight loss rate of the open and closed-type chambers.

facilitates the release of internal moisture and volatile components generated by water-rich condensate. At several time points, the closed-type sample showed slight apparent increases in weight compared to the previous measurement. These fluctuations were interpreted not as real material changes but as artifacts caused by environmental noise, such as external temperature fluctuations, air convection in the laboratory, or minor vibrations during high-temperature operation. Therefore, as shown in Fig. 4(c) and (d), the most representative parameter for assessing long-term thermal durability is considered to be the final weight loss measured after 1500 h, rather than the variations observed at intermediate time points. In previous weight-loss evaluations of commercially used neutron-shielding materials under open-type conditions at 170 °C for 1500 h, a weight loss of 3.535 wt% was reported [4]. In comparison, the weight loss of RNS-NR in this study was 1.380 wt% under identical conditions. This value is substantially lower than that of the commercial shielding resin and well within acceptable degradation limits, demonstrating that the developed neutron-shielding material satisfies the stability criteria and exhibits excellent long-term thermal performance.

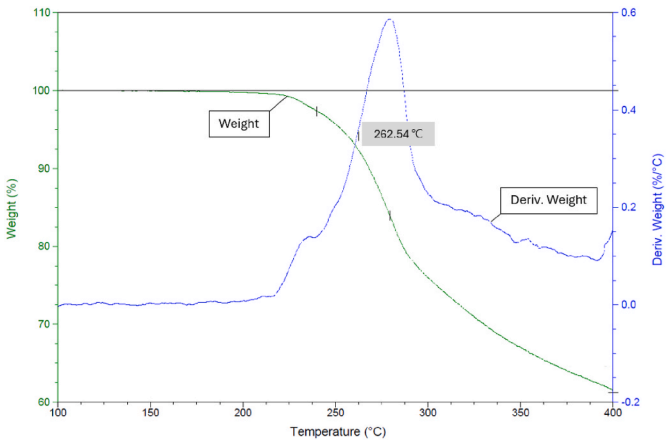

Fig. 5. Thermogravimetric analysis (TGA) and derivative weight curves of neutron-shielding resin (RNS-NR).

3.2. *Analysis of neutron-shielding resin after the long-term thermal test*

TGA results are presented in Fig. 5. The most pronounced weight change occurred at 262.54 °C, indicating that RNS-NR underwent major decomposition at this temperature. Similarly, the derivative thermogravimetric (DTG) curve, which represents the rate of mass loss with respect to temperature, showed its steepest slope at 262.54 °C and exhibited a distinct peak immediately thereafter. Notable weight loss was also observed above 200 °C, suggesting active thermal decomposition of the material under heating conditions. Although the extent of mass change in TGA measurements can be affected by heating rate and isothermal dwell time, the main purpose of this analysis was to determine the characteristic decomposition temperature. The long-term thermal exposure test conducted in this study was performed at 170 °C, which is significantly lower than the onset of major decomposition. Therefore, the gradual weight loss observed during the 1500 h exposure at 170 °C, as shown in Fig. 4, is interpreted not as a result of decomposition but as a minor reduction in mass due to gradual thermal aging and the release of water-rich condensate.

Fig. 6 presents the SEM micrograph and corresponding EDS elemental maps of the RNS-NR composite. The fractured cross section shows a heterogeneous microstructure in which inorganic fillers are embedded within the polymer matrix. The Al and O maps, which correspond primarily to the major filler $Al(OH)_3$, exhibit locally intensive regions that indicate the presence of relatively coarse $Al(OH)_3$-rich domains. This localized concentration is expected because $Al(OH)_3$ is the primary filler and is present at a substantially higher loading than the other additives. In contrast, the Zn and B maps show signals distributed broadly across the observed area without forming large, continuous clusters. These results suggest that the Zn and B containing fillers (zinc borate and boron carbide) are dispersed more finely and more uniformly within the matrix compared to the primary $Al(OH)_3$

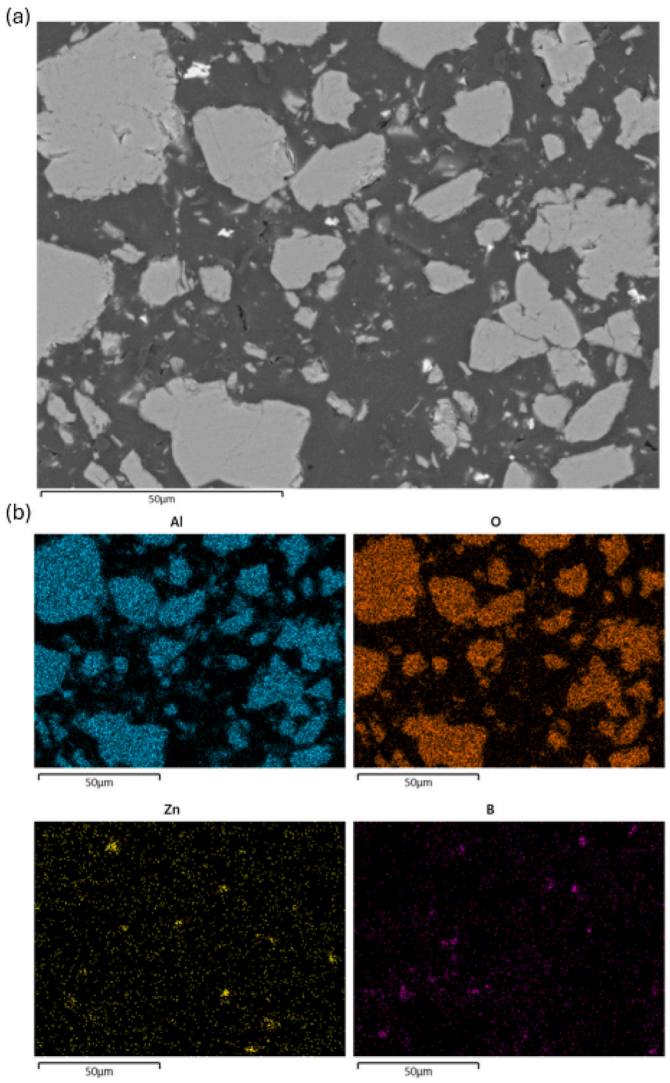

Fig. 6. (a) SEM micrograph of the cross section of RNS-NR; (b) EDS elemental maps showing the spatial distribution of Al, O, Zn, and B.

filler. Notably, the B signal showed broad distribution without forming large, continuous agglomerates at the SEM-EDS observation scale, and the accompanying Zn signal exhibited a similar spatial trend, suggesting co-distribution of Zn- and B-bearing fillers. Such suppression of large-scale agglomeration was commonly regarded as a favorable microstructural feature in shielding composites because well-dispersed functional fillers could increase effective radiation–material interaction within the matrix [9,10]. From a thermal durability perspective, the SEM-EDS results indicate a heterogeneous microstructure with filler-rich ($Al(OH)_3$) domains embedded in the polymer matrix, rather than complete uniformity. However, no evidence of large-scale segregation into distinct continuous layers is observed within the examined region, which suggests that the fillers remain sufficiently integrated to support the intended functional performance during long-term thermal exposure.

The XRD results are presented in Fig. 7. Specimens were sampled from three distinct regions within the resin block namely, the heater panel (nearest to the thermal source), the center (middle region), and the side (farthest from the heater). The diffraction patterns from all three positions exhibited nearly identical profiles, suggesting no significant structural transformation of the crystalline phase during the long-term thermal test. This finding indicates that the RNS-NR resin maintained its crystallographic integrity even after prolonged thermal exposure.

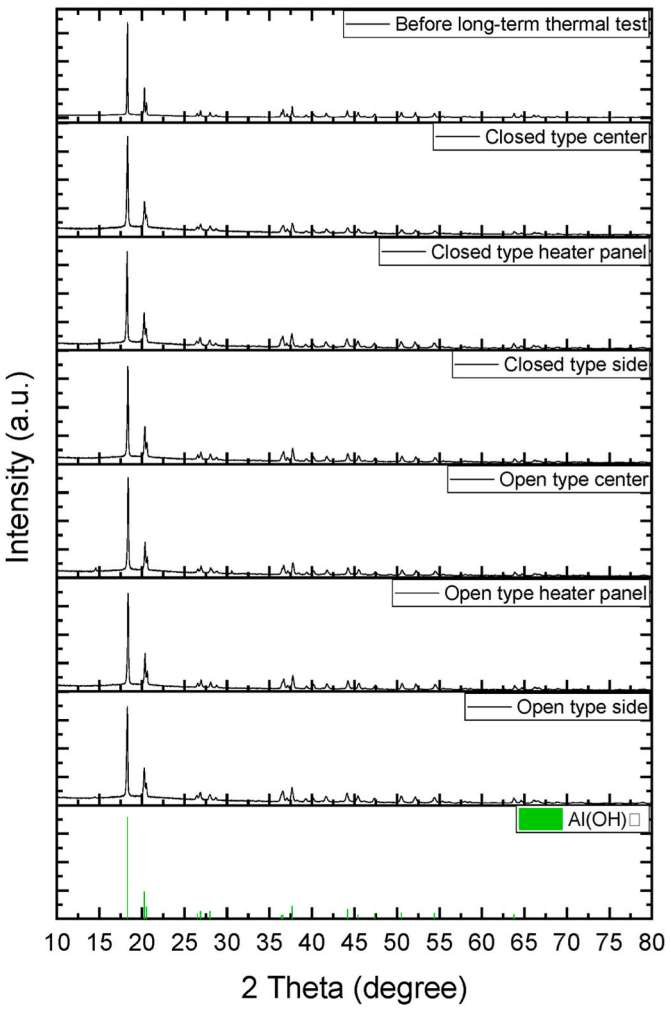

Fig. 7. XRD patterns of RNS-NR before the long-term thermal test and after thermal exposure in open-type and closed-type chambers at three sampling locations.

Notably, the primary filler component, aluminum hydroxide ($Al(OH)_3$), was consistently identified across all positions both before and after thermal aging. These results confirm that $Al(OH)_3$ remained chemically stable and did not undergo decomposition or phase transformation throughout the thermal durability test.

The water-rich condensate formed as droplets on the inner surface of the closed-type chamber, and a total of 3.67 g of condensate was collected for analysis. Because the available sample amount was limited, ICP-OES was used to identify inorganic elements potentially transferred into the condensed phase during the thermal test. ICP-OES analysis of the collected water-rich condensate detected boron at 17.6 ppm and zinc at 188 ppm, while aluminum was not detected. These results indicate that a minor fraction of boron containing species can transfer into a water-rich phase during thermal exposure. Based on the condensate results, the boron content of the solid resin was quantified at different locations using ICP-OES to evaluate location dependent boron retention after 2000 h of thermal aging at 170 °C. Zinc borate is sparingly soluble and undergoes hydrolysis at neutral pH, producing soluble boric acid and less soluble zinc hydroxide, which provides a plausible pathway for the simultaneous detection of boron and zinc in the condensate [24]. In this study, boron was prioritized for solid phase quantification because boron is the key neutron absorbing element that directly governs neutron shielding performance in boron based shielding systems [25,26]. Table 1 presents the initial boron concentration of 1.37 wt% and the final concentrations measured at the heater panel, center, and side

Table 1
Boron concentrations of neutron-shielding resin before and after the thermal test measured using ICP-OES.

Sample location	Initial B concentration (wt %)	Final B concentration (wt %)	Difference in B concentration (wt%)
Open-type heater panel	1.37	0.60	−0.77
Open-type center	1.37	0.46	−0.91
Open-type side	1.37	0.30	−1.07
Closed-type heater panel	1.37	0.48	−0.89
Closed-type center	1.37	0.31	−1.06
Closed-type side	1.37	0.31	−1.06

regions in both the open-type and closed-type chambers. For benchmarking, NS-4-FR used in licensed transport packages is specified to contain at least 1.444 wt% boron carbide, which corresponds to 1.13 wt % elemental boron [27]. The initial boron content of RNS-NR was 1.37 wt%, which is higher than the NS-4-FR elemental boron benchmark. In the open-type chamber, the final boron concentrations decreased with distance from the heater, from 0.60 wt% at the heater panel to 0.46 wt% at the center and 0.30 wt% at the side. In the closed-type chamber, the final boron concentration was 0.48 wt% at the heater panel and 0.31 wt % at both the center and side regions, which indicates similar boron depletion in the cooler regions under the enclosed atmosphere. The different spatial patterns between chamber types are consistent with moisture transport and contact conditions. In the open-type configuration, vapor is continuously vented and liquid water contact is minimized, so the boron profile more directly reflects the thermal gradient and shows progressive depletion toward the cooler side. In the closed-type configuration, water vapor is retained and repeatedly condenses as droplets on cooler surfaces, which can sustain aqueous contact and promote dissolution and redistribution of mobile boron species. Humidity can also promote boron mobilization from boron carbide through accelerated surface reactions that yield boric acid under humid atmospheres, which supports a moisture assisted pathway for boron transfer into a water-rich phase during prolonged exposure [28,29].

4. Conclusion

This study evaluated the long-term thermal durability of the neutron-shielding resin RNS-NR, developed for use in dry storage systems for spent nuclear fuel. Weight-loss monitoring revealed no abrupt reductions during the test period, with the closed-type sample exhibiting a total weight loss of 0.447 wt% and the open-type sample showing a loss of 1.380 wt%. The greater loss in the open-type sample was attributed to the continuous evaporation of water-rich condensate rather than polymer degradation. Supporting this interpretation, TGA analysis showed that major decomposition of the resin began at approximately 262.54 °C, which was well above the 170 °C exposure condition. This confirmed that the weight loss observed during thermal testing resulted from gradual moisture release rather than structural degradation. Furthermore, XRD analysis confirmed the retention of aluminum hydroxide before and after the 2000-h thermal test across different regions of the sample (heater panel, center, and side). Additionally, ICP-OES analysis of the water-rich condensate from the closed-type chamber identified boron at 17.6 ppm and zinc at 188 ppm while aluminum was not detected. These results indicate that a minor fraction of boron and zinc bearing species could be transferred into a condensed phase during heating. Consistent with this observation, ICP-OES analysis of solid samples collected after thermal exposure showed a decrease in boron content relative to the initial value of 1.37 wt%, with final values of 0.60, 0.46, and 0.30 wt% for the heater panel, center, and side regions in the open-type chamber and 0.48, 0.31, and 0.31 wt% in the closed-type chamber. These results demonstrate that the resin maintains thermal and structural stability under prolonged elevated-temperature conditions, while exhibiting measurable boron depletion and spatial variation that should be considered in long-term performance evaluation of neutron-shielding resins.

CRediT authorship contribution statement

Sia Hwang: Writing – review & editing, Writing – original draft, Visualization, Methodology, Investigation, Formal analysis, Conceptualization. **Tae Uk Kang:** Methodology, Investigation, Conceptualization. **Min Ji Kim:** Investigation. **Woo Jun Kang:** Methodology, Conceptualization. **Hee Reyoung Kim:** Writing – review & editing, Supervision, Conceptualization.

Declaration of competing interest

The authors declare that they have no known competing financial interests or personal relationships that could have appeared to influence the work reported in this paper.

Acknowledgements

This work was supported by the Korea Technology and Information Promotion Agency for SMEs(TIPA) and the Ministry of SMEs and Startups(MSS) (Grant no. S3373371) and the Korea Institute of Energy Technology Evaluation and Planning(KETEP) and the Ministry of Climate, Energy and Environment(MCEE) of the Republic of Korea (No. 20214000000410).

References

[1] Korea Hydro & Nuclear Power (KHNP), Status of spent nuclear fuel storage as of Q1 2025, in: KHNP Official Website, 2025. https://npp.khnp.co.kr/ON00400400300 6002/98990?blbrId=%EC%82%AC%EC%9A%A9%ED%9B%84%ED%95%B5%EC %97%B0%EB%A3%8C_1&searchType=TITLE&searchKeyword=&page=1. (Accessed 25 July 2025).
[2] J.G. Kim, Direction and challenges of high-level radioactive waste management – current status and future prospects of high-level radioactive waste management in Korea, Nuclear Industry 36 (6) (2016) 37–41.
[3] S.R. Greene, J.S. Medford, S.A. Macy, Storage and Transport Cask Data for Used Commercial Nuclear Fuel, DOE-Headquarters, 2013. ATI-TR-13047.
[4] N. Yamada, R. Asano, R. Horita, K. Kusunoki, Thermal behavior of neutron shielding material, NS-4-FR, under long term storage conditions, in: Proc. 14th Int. Symp. on the Packaging and Transportation of Radioactive Materials (PATRAM), Germany, Sep. 20–24, 2004.
[5] Korea Atomic Energy Research Institute, Development of Epoxy Nanocomposite Based Neutron Shielding Materials for Spent Fuel Cask, Ministry of Knowledge Economy, Korea, Jun, 2013. TRKO201400010624.
[6] U.S. Nuclear Regulatory Commission, Standard Review Plan for Spent Fuel Dry Storage Systems and Facilities – Final Report, U.S. Nuclear Regulatory Commission, Washington, DC, 2020. NUREG-2215.
[7] U.S. Nuclear Regulatory Commission, Standard Review Plan for Transportation Packages for Spent Fuel and Radioactive Material, U.S. Nuclear Regulatory Commission, Washington, DC, 2020. NUREG-2216.
[8] TA Instruments, Effect of Thermal Degradation on Polymer Thermal Properties, 2021. https://www.tainstruments.com/pdf/literature/TA430.pdf.
[9] Z. Huo, et al., Sm_2O_3 micron plates/B_4C/HDPE composites containing high specific surface area fillers for neutron and gamma-ray complex radiation shielding, Compos. Sci. Technol. 251 (2024) 110567.
[10] Z. Huo, et al., $PbWO_4$ micron spheres/B_4C/HDPE composites with different filler sizes for neutron and gamma ray shielding, Ceram. Int. 51 (2025) 55947–55958.
[11] Z. Huo, et al., Micromorphology tunable Eu_2O_3 submicron spheres reinforced boron-containing HDPE composites for neutron and gamma-ray complex radiation shielding, Ceram. Int. 51 (2025) 2360–2372.
[12] Z. Huo, et al., Microstructure regulatable $PbWO_4$ fillers reinforced B_4C/HDPE composites for synergistic radiation shielding of neutron and gamma-ray, Composites Part A 197 (2025) 109011.
[13] Center. Holtec, Holtec International Final Safety Analysis Report for the hi-storm 100 Cask System, NRC Agencywide Documents Access and Management System (ADAMS), 2010.

[14] H. Issard, Development of neutron shielding materials for high burn-up nuclear fuel storage facilities, in: International Association for Structural Mechanics in Reactor Technology (IASMiRT 20), Aug. 9–14, 2009.
[15] Y. Momma, M. Matsumoto, S. Shirai, O. Umegaki, Y. Irisa, K. Maruoka, K. Sakai, H. Nishioka, O. Kadota, Evaluation test on the thermal stability of resin as neutron shielding material for spent fuel transport cask, Int. Conf. Packag. Transp.Radioact. Mater. (PATRAM) (1998) 1645–1652.
[16] K.S. Bang, S.H. Yu, J.C. Lee, K.S. Seo, W.S. Choi, Thermal Test of KORAD-21 Cask, Korea Radioactive Waste Agency (KORAD), Korea, 2018, pp. 87–88.
[17] K. Ueki, et al., Shielding characteristics of neutron-shielding materials in a cask structure, Int. Conf. Packag. Transp.Radioact. Mater. (PATRAM) (1995) 1839–1846.
[18] Huber Advanced Materials, Halogen-free Fire Retardants and smoke suppressants in composite applications. https://www.huberadvancedmaterials.com/fileadmin/02_Solutions/_Brochures/Huber_Advanced_Materials_Halogen_Free_Fire_Retardants_for_Composites_v01.pdf. (Accessed 25 July 2025).
[19] Y. Li, L. Qi, Y. Liu, J. Qiao, M. Wang, X. Liu, S. Li, Recent advances in halogen-free flame retardants for polyolefin cable sheath materials, Polymers 14 (14) (2022) 2876.
[20] U.S. Borax, Firebrake® family of zinc borates: a guide to the firebrake ZB. https://www.borax.com/BoraxCorp/media/Borax-Main/Resources/Brochures/firebrake-family.pdf. (Accessed 25 July 2025).
[21] A. Alami, H. Issard, S. Momon, Development of Neutron Shielding Materials for transport/storage Casks and Installations, Institute of Nuclear Materials Management (INMM) Annual Meeting, 2011.
[22] K. Najima, H. Ohta, N. Ishihara, T. Matsuoka, S. Kuri, K. Ohsono, S. Hode, Development of neutron shielding material for cask, 9. International Conference on Nuclear Engineering, 2001.
[23] International Centre for Diffraction Data, PDF-4+ 2025 Database, ICDD, Newtown Square, PA, USA, 2025.
[24] D.M. Schubert, Zinc borate hydrolysis, Molecules 27 (18) (2022) 5768.
[25] Z. Qi, Z. Yang, J. Li, Y. Guo, G. Yang, Y. Yu, J. Zhang, The advancement of neutron-shielding materials for the transportation and storage of spent nuclear fuel, Materials 15 (9) (2022) 3255.
[26] M. Lovecký, J. Závorka, J. Jiřičková, Z. Ondráček, R. Škoda, Fixed neutron absorbers for improved nuclear safety and better economics in nuclear fuel storage, transport and disposal, Nucl. Eng. Technol. 55 (6) (2023) 2288–2297.
[27] Office for Nuclear Regulation (ONR), Certificate of Approval of Package Design GB/3516A/AF-96 (Rev.4) for Package Design GB/3516A, International Nuclear Services Limited, 2019.
[28] A. Kaitheri, J. Ofstad, E.A.C. Panduro, M. Oppegård, S.K. Padmanabhan, S. Pal, A. A. Licciulli, V. Johannesen, T. Eidet, K. Wiik, M.-A. Einarsrud, Evaluation of Boron Carbide powder stability under accelerated aging, Open Ceramics 22 (2025) 100755.
[29] P.D. Cuong, H.-S. Ahn, E.-S. Yoon, K.-H. Shin, Effects of relative humidity on tribological properties of boron carbide coating against steel, Surf. Coating. Technol. 201 (7) (2006) 4230–4235.